Progress In Electromagnetics Research, PIER 60, 19–41, 2006

APPLICATION OF PHYSICAL SPLINE FINITE ELEMENT METHOD (PSFEM) TO FULLWAVE ANALYSIS OF WAVEGUIDES

X. Zhou [†] **and G. Pan**

Department of Electrical Engineering
Arizona State University
Arizona, USA

Abstract—In this paper, the physical spline finite element method (PSFEM) is applied to the fullwave analysis of inhomogeneous waveguides. Combining (rectangular) edge element and the PSFEM, the cubic spline interpolation is successfully applied to the wave equation. For waveguide problems, the resulting nonlinear eigenvalue problem is solved by a simple iteration method in which the initial estimate is taken as the linear Lagrange interpolation, and then the solutions are improved by a few iterations. The bandwidth of the resultant matrix from the PSFEM is the same as that of linear Lagrange interpolation and is sparse. As a result, sparse matrix solver can be used. Three typical examples are demonstrated and compared with the analytical solutions and with the linear Lagrange interpolation results. It is observed that the present method converges much faster than the Lagrange interpolation method.

1. INTRODUCTION

In electromagnetics and microwave engineering, waveguide structures are important, both theoretically and practically. In theory, analytical solutions exist for many standard waveguides such as rectangular and circular metal waveguides, even for partially loaded dielectric waveguides. In applications, waveguides are basic components in microwave and optical networks. Therefore, the analysis of arbitrary waveguide structures has been a very active research topic for decades. Various techniques have been published, including separation of variables, conformal mapping, integral equation method, transmission

[†] X. Zhou is currently with Agere Systems Inc., 156 Wyndham Drive, Allentown, PA 18104, USA

line matrix (TLM), finite difference (FD), finite difference time-domain (FDTD), and finite element method (FEM). Among them, FEM is the most popular because of its solid mathematical foundation and flexibility in handling complicated geometries. The node-based FEM has been successfully applied to waveguide structures since 1960s [1]. Most important progresses are collected in a book [2]. In the 1980s, a "revolutionary" approach, edge (vector) element, was re-discovered. Its advantages have been recognized very soon in electromagnetics [3]. It can overcome all known drawbacks of FEM against other approaches. Especially, spurious (nonphysical) modes disappear naturally at all [4]. There is a trend that most authors are moving to the edge-based FEM. The commercial software package, Ansoft HFSS, is an edge based FEM tool. Attentions continue to be paid to efficiency and accuracy in more applications.

In either node-based or edge-based FEM, various orders of Lagrange interpolation are still dominating. Up to 8 order (p-element) Lagrange interpolation was implemented [5]. The implementation can be very difficult and inefficient. Furthermore, at the nodes or on the edges, discontinuous derivatives of fields still exist that may cause problems. One the other hand, spline interpolation has caught little attention. Very few articles of splines in FEM can be found [6], where only the B-spline was discussed. Because of the difficulty in implementation, spline functions have not been used in the FEM widely [7].

In recent papers [8, 9], a new finite element, physical spline finite element method (PSFEM), has been successfully developed and applied to one dimensional electromagnetic problems. The new interpolation greatly improves the accuracy and efficiency in one dimensional cases by incorporating physical equations into interpolations. However, in order to make the PSFEM practical in engineering, its extension to higher dimensions is necessary. In this paper, the PSFEM will be extended to a typical two-dimensional (2D) problem — the full wave analysis of waveguides. The initial results were shortly reported in [10]. The fundamental features introduced in PSFEM are described in [8, 9] in details, and will not be repeated here. The paper is organized as follows. Section 1 presents the functional for general waveguide problems. Section 2 reviews the edge finite element using the first order Lagrange interpolation. Section 3 applies the new physical spline finite element (PSFEM) to the edge finite element of waveguide problems. Section 4 describes a simple iteration algorithm for the resultant nonlinear eigenvalue problem. Three typical numerical examples are presented in Section 5 to show the effectiveness of the physical spline elements.

2. FUNCTIONAL FOR LOSSY, ANISOTROPIC WAVEGUIDE STRUCTURES

A general waveguide problem can be considered as a special case of structures with imperfectly conducting walls that are described mathematically by

$$\begin{aligned} \nabla \times \mathbf{E} &= -j\omega\mu\mathbf{H} && \text{(1a)} \\ \nabla \times \mathbf{H} &= j\omega\bar{\bar{\epsilon}} \cdot \mathbf{E} && \text{(1b)} \\ \nabla \cdot (\bar{\bar{\epsilon}} \cdot \mathbf{E}) &= \rho && \text{(1c)} \\ \nabla \cdot (\mu\mathbf{H}) &= 0 && \text{(1d)} \end{aligned}$$

in the finite computation region V. The boundary conditions are

$$\begin{aligned} \mathbf{n} \times \mathbf{E} &= \mathbf{P} \quad \text{on } S_1 && \text{(2a)} \\ \hat{n} \times \frac{1}{\mu_r} \nabla \times \mathbf{E} - \gamma_p \hat{n} \times \hat{n} \times \mathbf{E} &= \mathbf{U} \quad \text{on } S_2 && \text{(2b)} \end{aligned}$$

for the Dirichlet or Cauchy boundaries, where

$$\gamma_p = jk_0 \sqrt{\frac{\epsilon_{rc} - j\frac{\sigma}{\omega\epsilon_0}}{\mu_{rc}}}. \tag{3}$$

The functional is given as [11]

$$\begin{aligned} I &= \int_v \left[\frac{1}{\mu_r} (\nabla \times \mathbf{E}^a) \cdot (\nabla \times \mathbf{E}) - k_0^2 \mathbf{E}^a \cdot \bar{\bar{\epsilon_r}} \cdot \mathbf{E} \right] dv \\ &\quad + j\omega\mu_0 \int_v (\mathbf{J^e} \cdot \mathbf{E}^a + \mathbf{J^{e}}^a \cdot \mathbf{E}\ )\, dv \\ &\quad + \int_{s_2} (\mathbf{U} \cdot \mathbf{E}^a + \mathbf{U}^a \cdot \mathbf{E})\, ds - \int_{s_2} \gamma_p\, (\hat{n} \times \mathbf{E}^a) \cdot (\hat{n} \times \mathbf{E})\, ds \end{aligned} \tag{4}$$

where $\mathbf{E}^a$ is the testing field of $\mathbf{E}$. For waveguides, the special physical considerations are:

- integrals at two virtual end surfaces must vanish,
- For sources-free regions $\mathbf{J}_e = 0, \mathbf{J}_e^a = 0$,
- In most cases, we have $\mathbf{U} = 0, \mathbf{U}^a = 0$.

Based on the considerations above and the z-independent property, the functional on the cross section of a waveguide is

$$\begin{aligned} I_p &= \int \left[\frac{1}{\mu_r} (\nabla \times \mathbf{E}^a) \cdot (\nabla \times \mathbf{E}) - k_0^2 \mathbf{E}^a \cdot \bar{\bar{\epsilon}}_r \cdot \mathbf{E} \right] d\Omega \\ &\quad - \int_{l_2} \gamma_p\, (\hat{n} \times \mathbf{E}^a) \cdot (\hat{n} \times \mathbf{E})\, dl. \end{aligned} \tag{5}$$

Usually, the original field can be expressed as

$$\mathbf{E}(x,y,z) = (\mathbf{E}_t(x,y) + \hat{z}\mathbf{E}_z(x,y))e^{-\gamma z} \tag{6}$$

Obviously, it propagates in the positive z direction if the time convention is $e^{j\omega t}$. About the testing field, we have a few choices such as the original field itself [3], the complex conjugate of the original field, etc. However, the following is more convenient in our problem. The wave propagating in the negative z direction can be chosen as the adjoint field [12, 13]

$$\mathbf{E^a} = (\mathbf{E}_t - \hat{z}\mathbf{E}_z)e^{\gamma z}. \tag{7}$$

Because it is not a TEM wave, the z component ($\mathbf{E}_z \neq 0$) must be considered correctly. Separating the transverse and z component of the operator and using some vector identities, we arrive at

$$\begin{aligned}
(\nabla \times \mathbf{E}^a) \cdot (\nabla \times \mathbf{E}) &= (\nabla_t \times \mathbf{E}_t) \cdot (\nabla_t \times \mathbf{E}_t) \\
&\quad - (\gamma \mathbf{E}_t + \nabla_t E_z) \cdot (\gamma \mathbf{E}_t + \nabla_t E_z) \\
\mathbf{E}^a \cdot \bar{\bar{\epsilon}}_r \cdot \mathbf{E} &= \mathbf{E}_t \cdot \bar{\bar{\epsilon}}_{rz} \cdot \mathbf{E}_t - \bar{\bar{\epsilon}}_{rz} E_z^2 \\
(\hat{n} \times \mathbf{E}^a) \cdot (\hat{n} \times \mathbf{E}) &= (\hat{n} \times \mathbf{E}_t) \cdot (\hat{n} \times \mathbf{E}_t) - E_z^2.
\end{aligned} \tag{8}$$

Substituting (8) into (6), we have

$$\begin{aligned}
I_p &= \int \frac{1}{\mu_r} \left[(\nabla_t \times \mathbf{E}_t) \cdot (\nabla_t \times \mathbf{E}_t) \right] d\Omega \\
&\quad - \int_{l_2} \gamma_p \left[(\hat{n} \times \mathbf{E}_t) \cdot (\hat{n} \times \mathbf{E}_t) - E_z^2 \right] dl \\
&\quad - k_0^2 \int \left[\mathbf{E}_t \cdot \bar{\bar{\epsilon}}_{rz} \cdot \mathbf{E}_t - \bar{\bar{\epsilon}}_{rz} E_z^2 \right] d\Omega.
\end{aligned} \tag{9}$$

Mathematically, this functional can be discretized to yield a standard eigenvalue problem of k_0^2, provided γ is given. However, in waveguide case, we are mostly interested in finding the propagation constant γ itself. Then, we transfer the functional above into a desired form that can be discretized to a standard eigenvalue problem of γ, provided k_0 is given. Observing the γ term $(\gamma \mathbf{E}_t + \nabla_t E_z)$, if we set

$$\begin{aligned}
E_z &= \gamma e_z \\
\mathbf{E}_t &= \mathbf{e}_t
\end{aligned} \tag{10}$$

we can have

$$I_p = \int \left[\frac{1}{\mu_r} (\nabla_t \times \mathbf{e}_t) \cdot (\nabla_t \times \mathbf{e}_t) - k_0^2 \mathbf{e}_t \cdot \bar{\bar{\epsilon}}_{rt} \cdot \mathbf{e}_t \right] d\Omega$$
$$-\gamma^2 \left\{ \int \left[\frac{1}{\mu_r} (\mathbf{e}_t + \nabla_t e_z) \cdot (\mathbf{e}_t + \nabla_t e_z) - k_0^2 \bar{\bar{\epsilon}}_{rz} e_z^2 \right] d\Omega - \int_{l_2} \gamma_p e_z^2 dl \right\}$$
$$- \int_{l_2} \gamma_p (\hat{n} \times \mathbf{e}_t) \cdot (\hat{n} \times \mathbf{e}_t) \, dl. \tag{11}$$

3. REVIEW OF EDGE FEM

3.1. Lagrange Interpolation

The finite element method was early applied to structural engineering, especially scalar problems. So, traditional node expansions are created in a natural way. The method was not used in electromagnetics until 1968. The same node expansions are also invoked directly. However, contrary to what we expect, spurious mode unpredictably occurs in some cases [14]. Therefore, some approaches such as penalty function method have been proposed to suppress spurious modes [4]. From the mathematical point of view, this implies that the solution space must have been extended. In other words, some conditions (equations) are not considered correctly. Although the penalty terms can be added to the functionals to enforce the divergence conditions, they are cumbersome and unnatural. A natural way is to consider the divergence equations at the next stage, the construction of basic elements or interpolation functions. Traditional node based elements are discussed in details in [15]. It is shown that most node based elements do not satisfy the divergence equations. It is a good idea to incorporate vector properties of electromagnetic fields in constructing basic elements. These basic considerations lead to the so-called vector (edge) elements. Although vector elements were described forty years ago [16], they are noticed and used widely in electromagnetics until recently. In order to make some comments we summarize the construction of rectangular elements as follows.

Consider the rectangular element shown in Fig. 1. The side lengths are l_x and l_y in the x and y directions, respectively. The geometric center is (x_c, y_c). Decomposing the vector field (for example electric field) into x and y components, each component is one dimensional. The field at an arbitrary point (x, y) can be expressed in terms of the x and y components on the four edges. Suppose each field component varies linearly with respect to the related coordinates. Taking E_x as

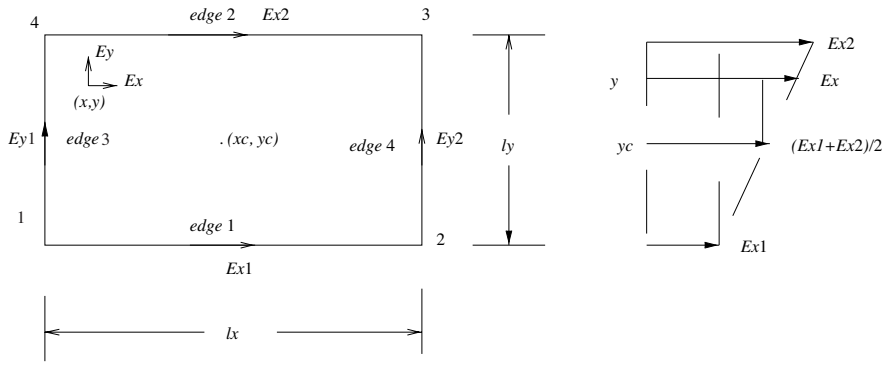

Figure 1. Rectangular edge element.

an example, from the geometric similarities shown in Fig. 1, we get

$$\frac{E_{x2} - E_{x1}}{l_y} = \frac{E_x - (E_{x1} + E_{x2})/2}{y - y_c}. \tag{12}$$

This equation can be simplified to the desired form, in terms of the x and y components on the edges as

$$E_x = \frac{1}{l_y}\left(y_c + \frac{l_y}{2} - y\right) E_{x1} + \frac{1}{l_y}\left(y - y_c + \frac{l_y}{2}\right) E_{x2} \tag{13}$$

which is independent of the x coordinate. Note that this does not mean the total field is independent of x because the y component E_y is a function of x. Eq. (13) is actually the first order (linear) Lagrange type interpolation.

In the same way, the y component can be expressed as

$$E_y = \frac{1}{l_x}\left(x_c + \frac{l_x}{2} - x\right) E_{y1} + \frac{1}{l_x}\left(x - x_c + \frac{l_x}{2}\right) E_{y2}. \tag{14}$$

If the edges are defined as shown in the figure, the field is expanded as

$$\mathbf{E} = \sum_{i=1}^{4} \mathbf{N_i} E_i \tag{15}$$

where only the tangential components E_i on the edges are required. The vector interpolations or basis functions are identified as

$$\mathbf{N}_1(y) \quad = \quad \frac{1}{l_y}\left(y_c + \frac{l_y}{2} - y\right)\hat{x}$$

$$\begin{aligned}
\mathbf{N}_2(y) &= \frac{1}{l_y}\left(y - y_c + \frac{l_y}{2}\right)\hat{x} \\
\mathbf{N}_3(x) &= \frac{1}{l_x}\left(x_c + \frac{l_x}{2} - x\right)\hat{y} \\
\mathbf{N}_4(x) &= \frac{1}{l_x}\left(x - x_c + \frac{l_x}{2}\right)\hat{y}.
\end{aligned} \tag{16}$$

The advantage is that each vector interpolation function consists of only a tangential component along the corresponding edge. So, the tangential continuity of the field across all edgeds is guaranteed automatically. The boundary conditions on the inner discontinuous interfaces can be included easily. Other more flexible shape elements are possible. They are needed when we want to model complicated structures. However, the interpolation above introduces implicitly another assumption: the $\mathbf{E_x}$ is a function of y only; the $\mathbf{E_y}$ is a function of x only. Or in general, all kinds of (first order) edge elements imply that the tangential components along any given edge are equal. This can be concluded directly from the expansions. Equivalently, the tangential components are the average values that are the unknowns in FEM. This assumption is not generally true in physics.

The vector basis functions above are used to expand transverse components in waveguide problems. For the longitudinal component, node-based interpolations are still needed. They are given as

$$\begin{aligned}
N_1(x,y) &= \frac{1}{l_x l_y}\left(x_c + \frac{l_x}{2} - x\right)\left(y_c + \frac{l_y}{2} - y\right) \\
N_2(x,y) &= \frac{1}{l_x l_y}\left(x - x_c + \frac{l_x}{2}\right)\left(y_c + \frac{l_y}{2} - y\right) \\
N_3(x,y) &= \frac{1}{l_x l_y}\left(x - x_c + \frac{l_x}{2}\right)\left(y - y_c + \frac{l_y}{2}\right) \\
N_4(x,y) &= \frac{1}{l_x l_y}\left(x_c + \frac{l_x}{2} - x\right)\left(y - y_c + \frac{l_y}{2}\right).
\end{aligned} \tag{17}$$

3.2. System Eigenvalue Problem

It is well known that based on the Lagrange interpolations, the functional (11) can be discretized to the following system eigenvalue problem

$$\begin{bmatrix} A_{tt} & 0 \\ 0 & 0 \end{bmatrix}\begin{bmatrix} e_t \\ e_z \end{bmatrix} = \gamma^2 \begin{bmatrix} B_{tt} & B_{tz} \\ B_{zt} & B_{zz} \end{bmatrix}\begin{bmatrix} e_t \\ e_z \end{bmatrix}. \tag{18}$$

Mathematically, it is a generalized eigenvalue problem

$$[A][X] = \lambda[B][X]. \tag{19}$$

3.3. Subspace Iteration Method

The most time-consuming part of FEM is the solution of the resultant matrix equations. In our case, it is the generalized eigenvalue problem (19). Two reasons indicate that the standard "dense" matrix methods can not be used. First, only the dominant and a few near-dominant waveguide modes are desired in practice. It is not necessary to solve all eigen values and eigenvectors since only those that are less than the testing frequency k_0 are physically meaningful. Secondly, the matrices $[A]$ and $[B]$ are usually large sparse if only first order Lagrange interpolation is employed. Therefore, sparse matrix techniques must be adopted. Subspace iteration method is one of the efficient sparse techniques. It is first proposed by K. Bathe [17]. Its applications to waveguide problems are described in [18, 19] and [20]. The procedure is summarized as follows

1. Choose initial vectors $[X^0]_{N\times p}$ and a shift η. Where N is the number of freedom of the problem ($p << N$).

2. Iterate

$$\begin{aligned} ([A]-\eta[B])\left[X^{s+1}\right] &= [B][X^s] \\ \left[A^{s+1}\right] &= \left[X^{s+1}\right]^T([A]-\eta[B])\left[X^{s+1}\right] \\ \left[B^{s+1}\right] &= \left[X^{s+1}\right][B]\left[X^{s+1}\right]. \end{aligned} \tag{20}$$

3. Stop the iterations by solving

$$\left[A^{s+1}\right]\left[U^{s+1}\right] = \left[B^{s+1}\right]\left[U^{s+1}\right]\left[\chi^{s+1}\right]. \tag{21}$$

4. ith ($i \le p$) eigenvalue is given by

$$\lambda_i^{s+1} = \chi_i^{s+1} + \eta \tag{22}$$

and eigenvector

$$\left[X^{s+1}\right] = \left[X^{s+1}\right]\left[U^{s+1}\right]. \tag{23}$$

5. Check the convergence

$$\left|\frac{\lambda_i^{s+1}-\lambda_i^s}{\lambda_i^{s+1}}\right| \le TOL \tag{24}$$

where TOL is a given tolerance.

Note that the costs of CUP time and memory are proportional to about $N^{1.5}$ and N respectively, if only one eigenvalue and its corresponding eigenvector are solved [19].

4. PSFEM IMPLEMENTATION

As we have done in one-dimensional problems [8, 9], Maxwell's equations can be embedded in the cubic splines to implement PSFEM. It is noted that in the edge element above, it is assumed implicitly that the x component of the field is independent of x, and the y component of the field is independent of y. That is, within an element

$$\mathbf{E}^e(x,y) = E_x^e(y)\hat{x} + E_y^e(x)\hat{y} + E_z^e(x,y)\hat{z}. \tag{25}$$

So the one-dimensional physical spline interpolation is applicable directly to $E_x^e(y)$ and $E_y^e(x)$.

4.1. Interpolation of Transverse Components

Let us consider non-magnetic materials with

$$\bar{\bar{\epsilon}}_r^e = \begin{bmatrix} \bar{\bar{\epsilon}}_{rxx}^e & 0 & 0 \\ 0 & \bar{\bar{\epsilon}}_{ryy}^e & 0 \\ 0 & 0 & \bar{\bar{\epsilon}}_{rzz}^e \end{bmatrix} \tag{26}$$

since general cases can be diagonalized [3, p.207] within an element. We have

$$\nabla^2 \mathbf{E}^e(x,y) = -k_0^2 \mu_r^e \bar{\bar{\epsilon}}_r^e \cdot \mathbf{E}^e(x,y). \tag{27}$$

Considering (25), we obtain

$$\frac{d^2 E_x^e(y)}{dy^2} = -(k_0^2 \mu_r^e \bar{\bar{\epsilon}}_{rxx}^e + \gamma^2) E_x^e(y) \tag{28a}$$

$$\frac{d^2 E_y^e(x)}{dx^2} = -(k_0^2 \mu_r^e \bar{\bar{\epsilon}}_{ryy}^e + \gamma^2) E_y^e(x) \tag{28b}$$

$$\nabla_t^2 E_z^e(x,y) = -(k_0^2 \mu_r^e \bar{\bar{\epsilon}}_{rzz}^e + \gamma^2) E_z^e(x,y). \tag{28c}$$

In terms of e_x, e_y, and e_z, they are

$$\frac{d^2 e_x^e(y)}{dy^2} = -(k_0^2 \mu_r^e \bar{\bar{\epsilon}}_{rxx}^e + \gamma^2) e_x^e(y) \tag{29a}$$

$$\frac{d^2 e_y^e(x)}{dx^2} = -(k_0^2 \mu_r^e \bar{\bar{\epsilon}}_{ryy}^e + \gamma^2) e_y^e(x) \tag{29b}$$

$$\nabla_t^2 e_z^e(x,y) = -(k_0^2 \mu_r^e \bar{\bar{\epsilon}}_{rzz}^e + \gamma^2) e_z^e(x,y). \tag{29c}$$

Expanding e_x and e_y using the one-dimensional physical splines yields the following field interpolations

$$\mathbf{e}_x^e(y) = \sum_{i=1}^{2} \left[(\mathbf{N}_i^e \cdot \hat{x}) - M_i^e (k_0^2 \mu_r^e \bar{\bar{\epsilon}}_{rxx}^e + \gamma^2) \right] e_x^e(y_i^e)\hat{x} \tag{30a}$$

$$\mathbf{e}_y^e(x) = \sum_{i=3}^{4} \left[(\mathbf{N}_i^e \cdot \hat{y}) - M_i^e (k_0^2 \mu_r^e \bar{\bar{\epsilon}}_{ryy}^e + \gamma^2) \right] e_y^e(x_i^e) \hat{y} \quad (30b)$$

where

$$M_i^e(y) = \frac{1}{6} \left[(\mathbf{N}_i^e \cdot \hat{x})^3 - (\mathbf{N}_i^e \cdot \hat{x}) \right] (l_y^e)^2, \quad (i = 1, 2) \quad (31a)$$

$$M_i^e(x) = \frac{1}{6} \left[(\mathbf{N}_i^e \cdot \hat{y})^3 - (\mathbf{N}_i^e \cdot \hat{y}) \right] (l_x^e)^2, \quad (i = 3, 4). \quad (31b)$$

To simplify the notation, let

$$p_x^e = -(k_0^2 \mu_r^e \bar{\bar{\epsilon}}_{rxx}^e + \gamma^2) \quad (32a)$$

$$p_y^e = -(k_0^2 \mu_r^e \bar{\bar{\epsilon}}_{ryy}^e + \gamma^2) \quad (32b)$$

and

$$\mathbf{B}_1^e(y) = \left[(\mathbf{N}_1^e \cdot \hat{x}) + M_1^e p_x^e \right] \hat{x} \quad (33a)$$

$$\mathbf{B}_2^e(y) = \left[(\mathbf{N}_2^e \cdot \hat{x}) + M_2^e p_x^e \right] \hat{x} \quad (33b)$$

$$\mathbf{B}_3^e(x) = \left[(\mathbf{N}_3^e \cdot \hat{y}) + M_3^e p_y^e \right] \hat{y} \quad (33c)$$

$$\mathbf{B}_4^e(x) = \left[(\mathbf{N}_4^e \cdot \hat{y}) + M_4^e p_y^e \right] \hat{y}. \quad (33d)$$

Then

$$\mathbf{e}_t^e(x, y) = \sum_{i=1}^{4} \mathbf{B}_i^e e_{ti}^e \quad (34)$$

which is similar to the traditional edge element interpolation (15).

4.2. Interpolation of Longitudinal Component

Next we need to consider interpolation of longitudinal component e_z. Similarly, it is easy to construct 2D PSFEM for a four node element as follows

$$e_z^e(x, y) = \sum_{i=1}^{4} B_i^e(x, y) e_{zi}^e \quad (35)$$

where the scalar complex expansion function is

$$B_i^e(x, y) = \left[N_i^e(x, y) + M_{zi}^e p_z^e \right]. \quad (36)$$

Considering the cubic splice requirements and $\nabla_t^2 = \partial^2/\partial x^2 + \partial^2/\partial y^2$, there is one and only one possible expansion of M_{zi}^e, which is

$$M_{zi}^e(x, y) = \frac{1}{6((l_x^e)^2 + (l_y^e)^2)} \left[(N_i^e)^3 - N_i^e \right] (l_x^e)^2 (l_y^e)^2, \quad (i = 1, 2, 3, 4) \quad (37)$$

and

$$p_z^e = -(k_0^2 \mu_r^e \bar{\epsilon}_{rzz}^e + \gamma^2). \tag{38}$$

4.3. Evaluation of Elemental Matrices

As usual, in the numerical implementation of finite element method, all elemental integrations must be evaluated based on the corresponding interpolations or expansions. In the PSFEM, the interpolations are described for rectangular elements. All matrices can be evaluated analytically in this case. Typical elemental matrices resulting from the discretization of the functional (11) contain the following integrals

$$E_{ij}^e = \int\int_{\Omega^e} (\nabla \times \mathbf{B}_i^e) \cdot \left(\nabla \times \mathbf{B}_j^e\right) d\Omega \tag{39a}$$

$$F_{ij}^e = \int\int_{\Omega^e} \mathbf{B}_i^e \cdot \mathbf{B}_j^e d\Omega \tag{39b}$$

$$G_{ij}^e = \int\int_{\Omega^e} \mathbf{B}_i^e \cdot \left(\nabla_t B_j^e\right) d\Omega \tag{39c}$$

$$H_{ij}^e = \int\int_{\Omega^e} (\nabla_t B_i^e) \cdot \left(\nabla_t B_j^e\right) d\Omega \tag{39d}$$

$$I_{ij}^e = \int\int_{\Omega^e} B_i^e B_j^e d\Omega. \tag{39e}$$

After tedious manipulations, the following analytical results are obtained

$$E_{11}^e = \frac{l_x^e}{l_y^e} + \frac{1}{45} p_x^2 l_x^e (l_y^e)^3 \tag{40a}$$

$$E_{12}^e = -\frac{l_x^e}{l_y^e} + \frac{7}{360} p_x^2 l_x^e (l_y^e)^3 \tag{40b}$$

$$E_{13}^e = -1 \tag{40c}$$

$$E_{14}^e = 1 \tag{40d}$$

$$E_{21}^e = E_{12}^e \tag{40e}$$

$$E_{22}^e = E_{11}^e \tag{40f}$$

$$E_{23}^e = 1 \tag{40g}$$

$$E_{24}^e = -1 \tag{40h}$$

$$E_{31}^e = -1 \tag{40i}$$

$$E_{32}^e = 1 \tag{40j}$$

$$E_{33}^e = \frac{l_y^e}{l_x^e} + \frac{1}{45} p_y^2 l_y^e (l_x^e)^3 \tag{40k}$$

$$E^e_{34} = -\frac{l^e_y}{l^e_x} + \frac{7}{360} p_y^2 l^e_y (l^e_x)^3 \quad (40l)$$
$$E^e_{41} = 1 \quad (40m)$$
$$E^e_{42} = -1 \quad (40n)$$
$$E^e_{43} = E^e_{34} \quad (40o)$$
$$E^e_{44} = E^e_{33} \quad (40p)$$

$$F^e_{11} = l^e_x l^e_y \left[\frac{1}{3} - \frac{2}{45}(l^e_y)^2 p_x \left(1 - \frac{1}{21}(l^e_y)^2 p_x\right)\right] \quad (41a)$$
$$F^e_{12} = l^e_x l^e_y \left[\frac{1}{6} - \frac{1}{180}(l^e_y)^2 p_x \left(7 - \frac{31}{84}(l^e_y)^2 p_x\right)\right] \quad (41b)$$
$$F^e_{13} = 0 \quad (41c)$$
$$F^e_{14} = 0 \quad (41d)$$
$$F^e_{21} = F^e_{12} \quad (41e)$$
$$F^e_{22} = F^e_{11} \quad (41f)$$
$$F^e_{23} = 0 \quad (41g)$$
$$F^e_{24} = 0 \quad (41h)$$
$$F^e_{31} = 0 \quad (41i)$$
$$F^e_{32} = 0 \quad (41j)$$
$$F^e_{33} = l^e_x l^e_y \left[\frac{1}{3} - \frac{2}{45}(l^e_x)^2 p_y \left(1 - \frac{1}{21}(l^e_x)^2 p_y\right)\right] \quad (41k)$$
$$F^e_{34} = l^e_x l^e_y \left[\frac{1}{6} - \frac{1}{180}(l^e_x)^2 p_y \left(7 - \frac{31}{84}(l^e_x)^2 p_y\right)\right] \quad (41l)$$
$$F^e_{41} = 0 \quad (41m)$$
$$F^e_{42} = 0 \quad (41n)$$
$$F^e_{43} = F^e_{34} \quad (41o)$$
$$F^e_{44} = F^e_{33} \quad (41p)$$

$$G^e_{11} = -\frac{1}{3} l^e_y + \frac{1}{45} l^e_y \left[(l^e_y)^2 p_x + t\left(1 - \frac{2}{21}(l^e_y)^2 p_x\right)\right] \quad (42a)$$
$$G^e_{12} = -G^e_{11} \quad (42b)$$
$$G^e_{13} = \frac{1}{6} l^e_y - \frac{1}{360} l^e_y \left[7(l^e_y)^2 p_x + t\left(7 - \frac{31}{42}(l^e_y)^2 p_x\right)\right] \quad (42c)$$
$$G^e_{14} = -G^e_{13} \quad (42d)$$
$$G^e_{21} = -G^e_{13} \quad (42e)$$
$$G^e_{22} = G^e_{13} \quad (42f)$$

$$G^e_{23} = -G^e_{11} \tag{42g}$$
$$G^e_{24} = G^e_{11} \tag{42h}$$
$$G^e_{31} = -\frac{1}{3}l^e_x + \frac{1}{45}l^e_x\left[(l^e_x)^2p_x + t\left(1 - \frac{2}{21}(l^e_x)^2p_x\right)\right] \tag{42i}$$
$$G^e_{32} = -\frac{1}{6}l^e_x + \frac{1}{360}l^e_x\left[7(l^e_x)^2p_x + t\left(7 - \frac{31}{42}(l^e_x)^2p_x\right)\right] \tag{42j}$$
$$G^e_{33} = -G^e_{32} \tag{42k}$$
$$G^e_{34} = -G^e_{31} \tag{42l}$$
$$G^e_{41} = G^e_{32} \tag{42m}$$
$$G^e_{42} = G^e_{31} \tag{42n}$$
$$G^e_{43} = G^e_{34} \tag{42o}$$
$$G^e_{44} = G^e_{33} \tag{42p}$$

$$H^e_{11} = \frac{1}{3}\left(\frac{l^e_y}{l^e_x} + \frac{l^e_x}{l^e_y}\right) - \frac{1}{9}l^e_x l^e_y p_z\left(\frac{2}{5} - \frac{1}{21}t\right) \tag{43a}$$
$$H^e_{12} = -\frac{1}{6}\left(\frac{2l^e_y}{l^e_x} - \frac{l^e_x}{l^e_y}\right) + \frac{1}{180}t\left[\left(\frac{8l^e_y}{l^e_x} - \frac{7l^e_x}{l^e_y}\right) + \frac{1}{420}t\left(\frac{167l^e_y}{l^e_x} + \frac{50l^e_x}{l^e_y}\right)\right] \tag{43b}$$
$$H^e_{13} = -\frac{1}{6}\left(\frac{l^e_y}{l^e_x} + \frac{l^e_x}{l^e_y}\right) + \frac{1}{180}l^e_x l^e_y p_z\left(7 - \frac{289}{840}t\right) \tag{43c}$$
$$H^e_{14} = -\frac{1}{6}\left(\frac{2l^e_x}{l^e_y} - \frac{l^e_y}{l^e_x}\right) + \frac{1}{180}t\left[\left(\frac{8l^e_x}{l^e_y} - \frac{7l^e_y}{l^e_x}\right) + \frac{1}{420}t\left(\frac{167l^e_x}{l^e_y} + \frac{50l^e_y}{l^e_x}\right)\right] \tag{43d}$$
$$H^e_{21} = H^e_{12} \tag{43e}$$
$$H^e_{22} = H^e_{11} \tag{43f}$$
$$H^e_{23} = H^e_{14} \tag{43g}$$
$$H^e_{24} = H^e_{13} \tag{43h}$$
$$H^e_{31} = H^e_{13} \tag{43i}$$
$$H^e_{32} = H^e_{23} \tag{43j}$$
$$H^e_{33} = H^e_{11} \tag{43k}$$
$$H^e_{34} = H^e_{12} \tag{43l}$$
$$H^e_{41} = H^e_{14} \tag{43m}$$

$$H^e_{42} = H^e_{24} \tag{43n}$$
$$H^e_{43} = H^e_{34} \tag{43o}$$
$$H^e_{44} = H^e_{11} \tag{43p}$$

$$I^e_{11} = l^e_x l^e_y \left[\frac{1}{9} - \frac{2}{675}t\left(8 - \frac{71}{147}t\right)\right] \tag{44a}$$
$$I^e_{12} = l^e_x l^e_y \left[\frac{1}{18} - \frac{1}{2700}t\left(41 - \frac{1613}{588}t\right)\right] \tag{44b}$$
$$I^e_{13} = l^e_x l^e_y \left[\frac{1}{36} - \frac{1}{10800}t\left(91 - \frac{4027}{588}t\right)\right] \tag{44c}$$
$$I^e_{14} = I^e_{12} \tag{44d}$$
$$I^e_{21} = I^e_{12} \tag{44e}$$
$$I^e_{22} = I^e_{11} \tag{44f}$$
$$I^e_{23} = I^e_{14} \tag{44g}$$
$$I^e_{24} = I^e_{13} \tag{44h}$$
$$I^e_{34} = I^e_{13} \tag{44i}$$
$$I^e_{32} = I^e_{23} \tag{44j}$$
$$I^e_{33} = I^e_{11} \tag{44k}$$
$$I^e_{34} = I^e_{12} \tag{44l}$$
$$I^e_{41} = I^e_{14} \tag{44m}$$
$$I^e_{42} = I^e_{24} \tag{44n}$$
$$I^e_{43} = I^e_{34} \tag{44o}$$
$$I^e_{44} = I^e_{33}. \tag{44p}$$

In all the formulas above

$$t = \frac{(l^e_x)^2 (l^e_x)^2}{(l^e_x)^2 + (l^e_x)^2} p_z. \tag{45}$$

Once these elemental matrices are evaluated, we are ready to solve the corresponding PSFEM problems. Because of the assumption (25), a factor of 0.5 is introduced in p_x and p_y of the G matrices. Obviously, if $p_x = p_y = p_z = 0$, all the matrices above reduce to the ones in the linear Lagrange elements.

5. ITERATION ALGORITHM FOR NONLINEAR EIGENVALUE PROBLEMS

It is easy to realize that the PSFEM results in a complicated eigenvalue problem. Since all elemental integrals or matrices are functions of

the unknown eigenvalue γ^2, the resulting problem is expected to be a nonlinear eigenvalue problem

$$[A(\lambda)][X] = \lambda[B(\lambda)][X]. \tag{46}$$

Strictly speaking, (46) is quite different from (19). It is generally difficult to solve the nonlinear eigenvalue problem (46) directly. The solution of (46) type problem is still an active research interest in mathematics [21]. Fortunately, we developed the following iteration algorithm to overcome this difficulty.

1. Use the traditional Lagrange interpolation solution with course mesh as the initial values for eigenvalues and fields. That is to solve (19) as initial values for the following iterations.

2. Iterate

$$[A(\lambda^{(s)})][X] = \lambda^{(s+1)}[B(\lambda^{(s)})][X]. \tag{47}$$

Eq. (47) is a regular generalized eigenvalue problem. Then the same subspace iteration method describe in Section 3.3 can be used to solve (47) in each iteration. It is found that only two or three iterations result in convergent eigenvalues in practice.

6. NUMERICAL EXPERIMENTS

Any numerical techniques must be verified with numerical experiments. The attractive effects of the PSFEM in analysis of waveguide structures will be tested in this section. Three classical examples are employed to emphasize various aspects of the PSFEM. It is a good thing that analytical solutions exist in all three examples, then the comparisons are reliable.

6.1. A Standard Rectangular Waveguide

A rectangular air filled waveguide is used to demonstrate the suppression of spurious modes using edge elements. The cutoff wavenumber of a rectangular waveguide of dimensions a and b is given by [22]

$$\begin{aligned} \frac{k_c^{TE}}{k_{c10}} &= \sqrt{m^2 + \left(\frac{na}{b}\right)^2} \\ m &= 0, 1, 2, \ldots \quad n = 0, 1, 2, \ldots. \quad m = n \neq 0 \end{aligned}$$

for TE modes, and

$$\frac{k_c^{TM}}{k_{c10}} = \sqrt{m^2 + \left(\frac{na}{b}\right)^2} \quad m = 1, 2, \ldots \quad n = 1, 2, \ldots.$$

for TM modes. The first ten modes for both TE and TM modes are listed in the TABLE 8.1 and TABLE 8.2 of [22]. Table 1 compares our results for the first five modes with analytical ones and the results obtained by the existing edge element FEM (Lagrange interpolation) and the PSFEM. N is the number of uniform elements in each direction. The computation frequency is 200 MHz. An excellent agreement has been observed. No spurious mode appears. Notice that TE_{11} and TM_{11} modes should be degenerate. However, Lagrange FEM yields some difference. The PSFEM converges to the same up to 9th decimal. Table 2 illustrates the convergence of the two methods for the fundamental mode TE_{10}. It is immediately concluded that the PSFEM converges much faster. Even in the extreme case, with only 2×2 mesh, the PSFEM works well while the Lagrange FEM does not. Equivalently, the PSFEM saves a lot of computation time.

Table 1. Comparison of cutoff wavenumber of a rectangular waveguide.

Modes	k_c				
	Analytical	PSFEM		Lagrange	
		N=10	N=30	N=10	N=30
TE_{10}	1.396263402	1.396262944	1.396262382	1.40201115	1.396900458
TE_{20}	2.792526803	2.792594618	2.792526256	2.838658747	2.797632829
TE_{01}	3.141592654	3.141593262	3.141592008	3.154526737	3.143027678
TE_{11}	3.437899924	3.442959083	3.438510391	3.452059993	3.439470449
TM_{11}	3.437899924	3.442959083	3.438510391	3.452054346	3.439476812

Table 2. Comparison of convergence of two methods for TE_{10} mode of a rectangular waveguide with $a/b = 2.25$.

N	k_c		percentage error	
	PSFEM	Lagrange	PSFEM	Lagrange
2(minimum)	1.402680591	1.539599762	0.460%	10.266%
3	1.396930044	1.460592495	0.048%	4.607%
6	1.396274055	1.412261944	0.001%	1.146%
9	1.396263434	1.403361534	0.000%	0.508%
12	1.396262572	1.400253158	0.000%	0.286%
15	1.396262433	1.398815719	0.000%	0.183%
18		1.398035243		0.127%
21		1.397564762		0.093%
24		1.397259452		0.071%

Table 3. Comparison of convergence of three methods for the fundamental mode of a partially dielectric filled rectangular waveguide with, $\epsilon_r = 2.45, a/b = 0.45, d/a = 0.50$.

Frequency ($10^8 Hz$)	a/λ_0	k_z/k_0			Error%	
		Analytical	PSFEM	Lagrange	PSFEM	Lagrange
1.200000	0.180125	0.000000	0.000002	0.000003		
1.288889	0.193467	0.354678	0.355883	0.329029	0.340	7.232
1.377778	0.206810	0.551107	0.551836	0.536975	0.132	2.564
1.466667	0.220152	0.672805	0.673364	0.662616	0.083	1.514
1.555556	0.233495	0.761098	0.761560	0.753081	0.061	1.053
1.644444	0.246837	0.829714	0.830108	0.823109	0.048	0.796
1.733333	0.260180	0.885326	0.885669	0.879724	0.039	0.633
1.822222	0.273523	0.931771	0.932073	0.926919	0.032	0.521
1.911111	0.286865	0.971476	0.971744	0.967205	0.028	0.440
2.000000	0.300208	1.006075	1.006313	1.002264	0.024	0.379

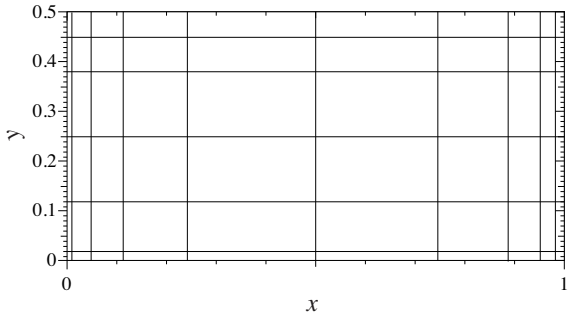

Figure 2. Discretization of a rectangular waveguide.

6.2. A Lossy Dielectric Waveguide

A rectangular metallic filled with homogeneous, isotropic and lossy dielectric is solved. In this case, we have the exact analytic solution of the propagation constant [23]

$$\gamma = \alpha + j\beta = k_0 \sqrt{\left(\frac{m\pi}{k_0 a}\right)^2 + \left(\frac{n\pi}{k_0 b}\right)^2 - \epsilon_r} \tag{48}$$

where m and n are the mode indices for the x and y directions.
The discretization of the structure is shown in Fig. 2. Only 10×10 nonuniform meshes in geometric progression (1×0.5) in each direction

are used to demonstrate the numerical computations. The relative dielectric constant is

$$\epsilon_r = 4 - j100.$$

The numerical and analytic results of the attenuation constant and phase constant of the dominate mode TE_{10} are compared in Fig. 3 and Fig. 4, respectively. It is seen that the PSFEM works very well in lossy cases.

6.3. A Partially Dielectric-Filled Waveguide

The structure is shown in Fig. 5. This is another well-known test problem of numerical techniques for waveguide structures. It is first solved analytically by L. Pincherle [24] and then cited in [12, 22, 25].

The propagation constant for $TM^x(LSM^x)$ is determined by [25]

$$k_{x1}^2 + \left(\frac{n\pi}{b}\right)^2 + k_z^2 = \omega^2\epsilon_1\mu_1 \tag{49a}$$

$$k_{x2}^2 + \left(\frac{n\pi}{b}\right)^2 + k_z^2 = \omega^2\epsilon_2\mu_2 \tag{49b}$$

and the transcendental equation

$$\frac{k_{x1}}{\epsilon_1}\tan k_{x1}d + \frac{k_{x2}}{\epsilon_2}\tan k_{x2}(a-d) = 0 \tag{50}$$

For $TE^x(LSE^x)$ mode, (50) is replaced by

$$\frac{k_{x1}}{\epsilon_1}\cot k_{x1}d + \frac{k_{x2}}{\epsilon_2}\cot k_{x2}(a-d) = 0. \tag{51}$$

Similar structures are solved using FEM in [26–28] etc. In order to be comparable with existing literature, the same structure used in [25, p.161] is solved here using analytical, PSFEM and Lagrange FEM. Fig. 6 shows the results for the first three modes. Notice that from the present results, the curve given in Fig. 4–7 of [25] may not be accurate enough. For example, at $a/\lambda_0 = 0.3$, k_z/k_0 is a little bit less than 1.0 in [25], but the present analytic calculation is a little bit greater than 1.0. The analytical results are verified with several math tools. The curve in [25] is after earlier computation of N. H. Frank, it is possible that the solution of the transcendental equations was not accurate enough at that time. A copy can be found in [29, p.393].

It can be seen clearly that the PSFEM results are in better agreement with the analytical solution. To emphasize this point, numerical data are listed in Table 3. Again the PSFEM converges much faster than the traditional FEM does.

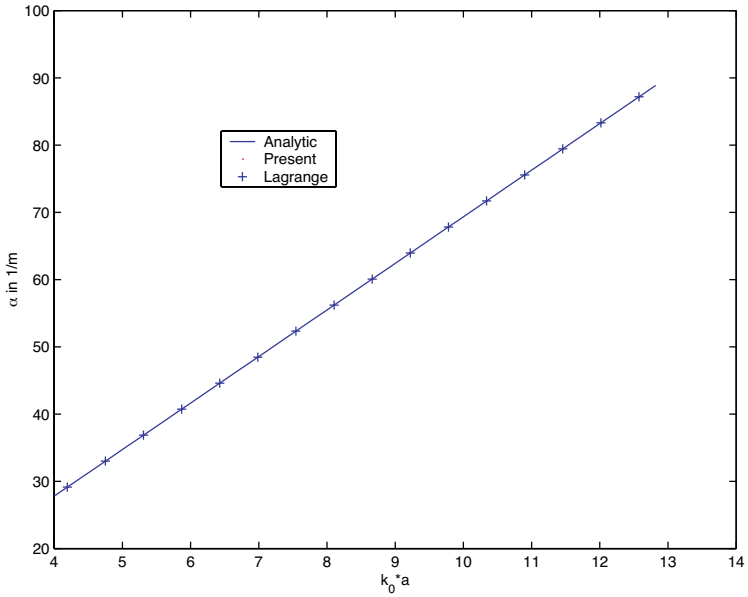

Figure 3. Attenuation of the lossy dielectric-loaded waveguide.

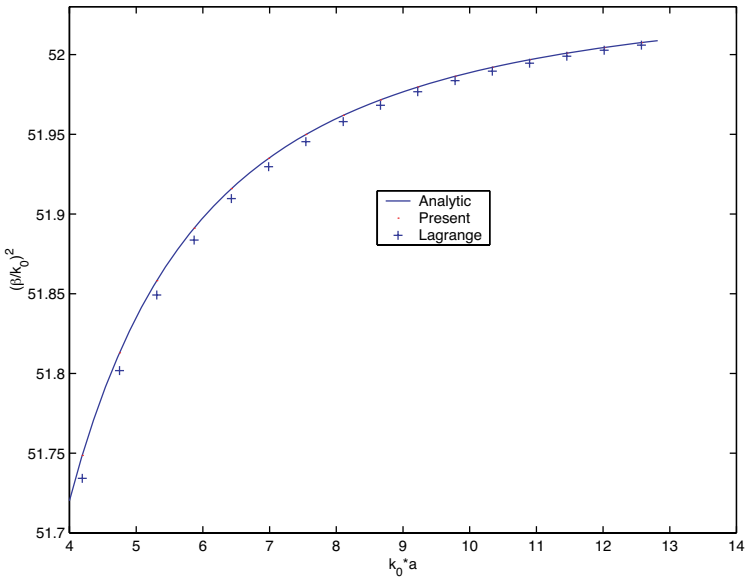

Figure 4. Dispersion of a lossy dielectric-loaded waveguide.

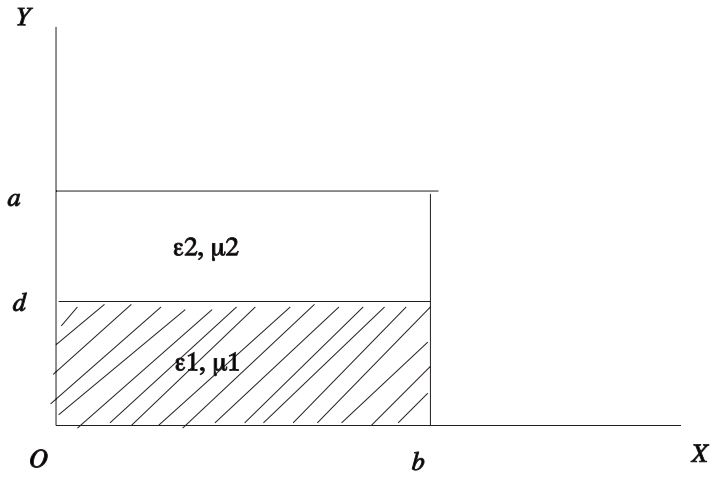

Figure 5. Description of a partially dielectric-filled waveguide.

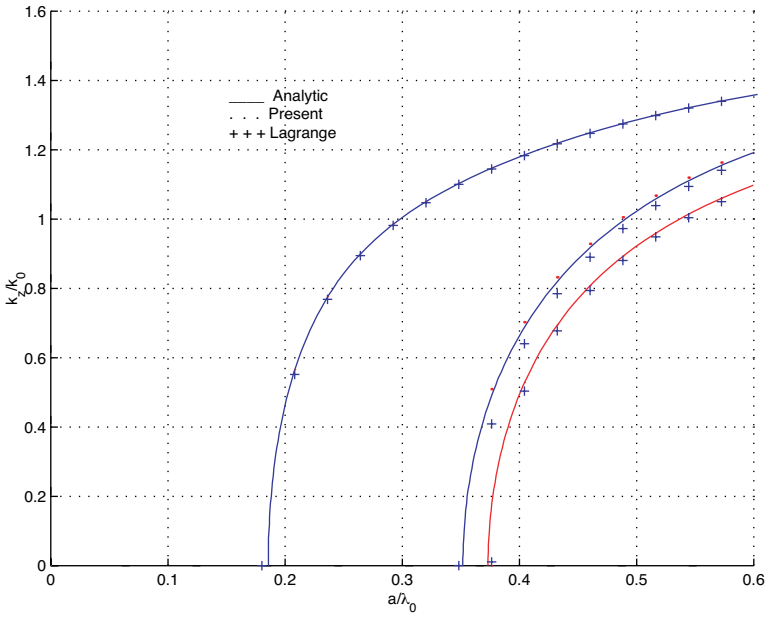

Figure 6. Propagation constant for the first three modes of a partially dielectric filled rectangular waveguide with, $\epsilon_r = 2.45$, $a/b = 0.45$, $d/a = 0.50$.

7. CONCLUSION

The physical spline finite element method (PSFEM) is successfully extended to 2D electromagnetic problems, namely, the full wave analysis of waveguides. The corresponding system matrix has the same bandwidth as the linear Lagrange elements. However, the convergence and accuracy are improved significantly. The implementation shows the usefulness of PSFEM in electromagnetic engineering. In waveguide problems, the resultant nonlinear eigenvalue problem is very challenging. New algorithms for solving it are needed. On the other hand, it is worthwhile to extend the PSFEM to 3D guided wave cases and to scattering and radiation problems.

REFERENCES

1. Silvester, P., "Finite-element solution of homogeneous waveguide problems," *Alta Frequenza,* Vol. 38, 313–317, 1969.
2. Silvester, P. P. and G. Pelosi, *Finite Elements for Wave Electromagnetics: Method and Techniques,* IEEE Press, New York, 1994.
3. Jin, J., *The Finite Element Method in Electromagnetics,* John Wiley & Sons, New York, 1993.
4. Paulsen, K. D. and D. R. Lynch, "Elimination of vector parasites in finite element Maxwell solutions," *IEEE Trans. Microwave Theory and Tech.,* Vol. 39, 395–404, 1991.
5. Webb, J. P. and B. Forghani, "Hierarchal scalar and vector tetrahedra," *IEEE Trans. on Magnetics,* Vol. 29, 1495–1498, Mar. 1993.
6. Liang, X., B. Jian, and G. Ni, "The B-spline finite element method in electromagnetic field numerical analysis," *IEEE Trans. on Magnetics,* Vol. MAG-23, 2641–2643, Sept. 1987.
7. Mitchell, A. R., "Variational principles and the finite element method," *J. Inst. Maths. Applic.,* Vol. 9, 378–389, 1972.
8. Zhou, X., "Physical spline finite element (PSFEM) solutions to one dimensional electromagnetic problems (abstract)," *J. of Electromagn. Waves and Appl.,* Vol. 17, No. 8, 1159–1160, 2003.
9. Zhou, X., "Physical spline finite element (PSFEM) solutions to one dimensional electromagnetic problems," *Progress in Electromagnetics Research, PIER,* Vol. 40, 271–294, 2003. http://cetaweb.mit.edu/pier/pier40/pier40.html.
10. Zhou, X. and G. Pan, "Application of physical spline FEM to

waveguide problems," *PIERS 2000 Progress in Electromagnetics Research Symposium, Proceedings*, 77, Boston, USA, July, 2002.

11. Pan, G. and J. Tan, "General edge element approach to lossy and dispersive structures in anisotropic media," *IEE Proc. - Microw. Antennas Propag.,* Vol. 144, 81–90, April 1997.
12. Collin, R. E., *Field Theory of Guided Waves,* IEEE Press, New York, 1991.
13. Jackson, J. D., *Classical Electrodynamics,* John Wiley & Sons, New York, 1975.
14. Crowley, C. W., P. P. Silvester, and H. Hurwitz, "Covariant projection elements for 3D vector field problems," *IEEE Trans. Magnetics,* Vol. 24, 397–400, 1988.
15. Silvester, P. P., *Finite Elements for Electrical Engineers,* Cambridge University Press, New York, 1990.
16. Whitney, H., *Geometric Integration Theory,* Princeton University Press, Princeton, NJ, 1957.
17. Bathe, K. J. and E. L. Wilson, *Numerical Methods in Finite Element Analysis,* Prentice-Hall, Inc., New Jersey, 1976.
18. Fernandez, F. A., J. B. Davies, S. Zhu, and Y. Lu, "Sparse matrix eigenvalue solver for finite element solution of dielectric waveguides," *Electronics Letters,* Vol. 27, 1824–1826, Sept. 1991.
19. Lu, Y., "The efficient solution of large sparse nonsymmetric and complex eigensystems by subspace iteration," *IEEE Trans. on Magnetics,* Vol. 30, 3582–3585, Sept. 1994.
20. Tan, J. and G. Pan, "A new edge element analysis of dispersive waveguiding structures," *IEEE Trans. Microwave Theory and Tech.,* Vol. 43, 2600–2607, Nov. 1995.
21. Guillaume, P., "Nonlinear eigenproblems," *SIAM J. Matrix Anal. Appl.,* Vol. 20, 575–595, Mar. 1999.
22. Balanis, C. A., *Advanced Engineering Electromagnetics,* John Wiley & Sons, New York, 1989.
23. Lu, Y. and A. Fernandez, "An efficient finite element solution of inhomogeneous anisotropic and lossy dielectric waveguides," *IEEE Trans. Microwave Theory and Tech.,* Vol. 41, 1215–1223, June–July 1995.
24. Pincherle, L., "Electromagnetic waves in metal tubes filled longitudinally with two dielectrics," *Physical Review*, Vol. 66, 118–130, Sept. 1944.
25. Harrington, R. F., *Time-Harmonic Electromagnetic Fields,* McGraw-Hill, Inc., New York, 1961.
26. Hano, M., "Finite-element analysis of dielectric-loaded waveg-

uides," *IEEE Trans. Microwave Theory Tech.,* Vol. MTT-32, 1275–1279, Oct. 1984.

27. Koshiba, M., K. Hayata, and M. Suzuki, "Finite-element formulation in terms of the electric-field vector for electromagnetic waveguide problems," *IEEE Trans. Microwave Theory Tech.,* Vol. MTT-33, 900–905, Oct. 1985.
28. Bárdi, I. and O. Bíró, "Improved finite element formulation for dielectric loaded waveguides," *IEEE Trans. on Magnetics,* Vol. 26, 448–453, Mar. 1990.
29. Marcuvitz, N., *Waveguide Handbook,* Peter Peregrinus Ltd, New York, 1985.